Voltage Control of Critical and Non-Critical Loads in Distribution Networks with Electric Spring

Mohammad Askarpour[a], Jamshid Aghaei[a], Mohammad Hassan Khooban[b], Miadreza Shafie-khah[c], and João P. S. Catalão[d, *]

[a] *Department of Electrical and Electronics Engineering, Shiraz University of Technology, Shiraz, Iran (e-mail: m.askarpour@sutech.ac.ir, aghaei@sutech.ac.ir)*
[b] *Department of Engineering, Aarhus University, Inge Lenhmanns Gade 10, 8000 Aarhus C, Denmark (khooban@eng.au.dk)*
[c] *School of Technology and Innovations, University of Vaasa, 65200 Vaasa, Finland (mshafiek@uva.fi)*
[d] *Faculty of Engineering of the University of Porto and INESC TEC, Porto 4200-465, Portugal (catalao@fe.up.pt)*

[*] *Corresponding Author*: J. P. S. Catalão *(catalao@fe.up.pt)*

Abstract — The electric spring (ES) is a novel voltage compensator which is series with a non-critical load to regulate the critical load voltage. The voltage fluctuation is caused by wind speed fluctuation, load fluctuation, and generator tripping. In busbar voltage drop situation, the electric spring decreases the voltage of non-critical load in order to support the critical load (busbar) voltage. All the non-critical loads couldn't work under any voltage (for example 0.5pu). In this paper, a control strategy founded on active and reactive power compensations has been proposed for voltage control of critical loads on a reference value while it controls the voltage of non-critical loads between an acceptable boundary. The proposed controller has two voltage control loops which adjusts active and reactive power of the electric spring. The experimental results from the case study show that the ES with the proposed control strategy can effectively mitigate double voltage control of both critical and non-critical loads while dynamically managing the demand response of the system at the same time.

Keywords — Active and reactive power control; Electric spring; Double voltage control, Distribution networks; Critical loads; Non-critical loads.

1. List of Symbols

P_{in} Total critical and noncritical active powers

P_0 Active power of noncritical load

P_1 Active power of critical load

V_s Critical load voltage vector (busbar or mains voltage)

V_0 Noncritical load voltage vector

V_{es} Electric spring voltage vector

Z_1 Impedance of critical load

Z_0 Impedance of noncritical load

R_1 Resistance of critical load

R_0 Resistance of noncritical load

2. Introduction

2.1. Motivation and Aims

Growing penetration of renewable energy sources (RESs) such as wind power generation and photovoltaics will impose new challenges to the future power systems. Owing to the spatially distributed and intermittent characteristics of RESs, it is not straightforward to predict and control the total power generation instantaneously [1]. Increasing intermittent renewable energy sources could destabilize the ac mains voltage. Different methods have been used to control the distribution network voltage recently [2]–[6].

In the RES-integrated power systems, a new control mechanism is essential to guarantee that the load demand will follow the undispatchable power generation pattern by RESs [7], [8], which is in contrast with the traditional power systems where the generation side should follow the load demand. To achieve this goal, the demand-side management methods are studied. They can be

categorized in four branches:1) scheduling of daily tasks of variable power demands [9]–[11]; 2) real-time pricing [12]–[14]; 3) demand peak shaving using energy storage systems [15]; and 4) remote control (on–off) of smart loads [16]–[18]. The first and second methods are well suited to adapt the load profiles based on a predetermined behavior. However, they are not good options to make real time balance between generation and loads. The third approach is an appropriate solution to cope with the real time power imbalances but it does not have adequate capacity and it is an expensive solution. The fourth method can satisfy the real-time power balance, but it is an unpleasant method for consumers. The last two methods are fast solutions which satisfy the instantaneous power balance.

Electric spring (ES) is designed to support the AC voltage of critical load and let the voltage of non-critical load to fluctuate. The ES and non-critical load are connected in series. With injecting/absorbing reactive power, the ES regulates the voltage of critical load. In this paper, the double voltage control is implemented to control both load voltages in distributed networks or microgrid in grid connected mode. This control strategy uses an active and reactive power compensation to accomplish this control scheme.

2.2. Literature Overview

There are conventional means to overcome microgrid problems such as control and architecture, power compensation, power factor and power quality improvement. Ref. [19] has suggested a hybrid ac/dc microgrid architecture for smart building to increase the penetration of DGs and to isolate the interference to the grid. There are some new control strategies for DC microgrid architecture. Scalable and controllable dc microgrid architecture has been presented with a source-end to load-end one-way communication in [20] and with phase shifted full bridge in [21]. In Ref. [22] design metrics and performance evaluation of a scalable DC microgrid are documented with

a look-up table for generated power of a source converter. In [23], a coordinated harmonic compensation and voltage support strategy is presented for distributed generations' interface inverters in a grid-connected microgrid. A unified design and implementation of active power filters (APF) for medium-voltage high-power applications is presented in [24]. In [25], optimal active and reactive power compensation was performed on a continuously loaded power system, using the battery energy storage system. A novel solution of power quality management for the photovoltaic (PV) power plant with the transformer integrated filtering method is presented in [26]. The references [27] and [28] propose different approaches to utilizing Buck converter as a Power Factor Correction (PFC) controller. The reference [29] proposes a design of an efficient adaptive neural-fuzzy inference system-based voltage controller for active power factor correction.

Electric spring with reactive power compensation can set the bus voltage to one per-unit [30]. Therefore, ES can stabilize the bus voltage and correct the power factor. These research topics are the aims of papers [31] & [32]. Mok et al. [33] have introduced Electric spring to DC distribution system to solve the problem of bus voltage instability, voltage droop, system fault and harmonics. Control of ES is another important issue especially when there are a lot of electric springs distributed along the network. Chaudhuri [34] has proposed a droop control for ESs in a distribution network.

The papers [35] and [36] have also suggested different distributed control strategies for multiple electric springs. Another interesting implementation of ES is for power imbalance reduction in three phase imbalanced power system [37]. The last research topic is concentrated on battery management [38]-[39]. The paper [40] has showed with using ES the energy storage requirement is reduced significantly. Reference [39] has used ES with coordinated battery management for reducing voltage and frequency fluctuations in microgrid in islanded mode.

All of the above papers with different research topics could be classified from another viewpoint; which is the type of the ES compensation modes. The critical voltage stabilizing and power factor correction could be classified in reactive power compensation. The frequency stabilizing is accomplished with the active power compensation. Most of the above papers have utilized reactive power compensation.

Papers [39] and [41] have employed both active and reactive power compensations to overcome both voltage and frequency fluctuation problems in islanded microgrids. Actually, when a microgrid is in the grid-connected mode the small active power injection of the electric spring can't change the frequency of the power system therefore in this mode the frequency is considered to be fixed. That's why there is no active power compensation for frequency stabilization in grid-connected mode but there is for islanded mode.

This paper proposes a control strategy for ES with active and reactive power compensations for active distribution networks or microgrids in grid-connected mode. The proposed control strategy utilizes the reactive power compensation to control the critical load voltage and active power compensation to control the noncritical load voltage.

2.3. Features and Capabilities

The electric spring is a series compensator. The circuit block diagram is shown in Fig. 1. For reactive power compensation, ES has produced a voltage (v_{es}) which is perpendicular to the current of non-critical load (i_o). When a voltage drop is happened in the power system, the voltage of ES is increased so the voltage and power of non-critical load (v_o) is decreased until the voltage of critical load (mains voltage v_s) is reached to one per-unit. The question here is; does the non-critical load work with any voltage? Definitely not. How much voltage reduction could be

acceptable? It depends on the type of non-critical load. Example of non-critical loads include electric water heaters, refrigerators, and lightening systems [42].

Let's assume non-critical load is an electrical bulb (lamp). If it is connected to 220 volts (one per-unit), the output power will be one per-unit. If it is connected to 0.9 per-unit voltage, the output power will be approximately 0.8 per-unit. If it is connected to 0.5 per-unit voltage, the output power will be 0.25 per-unit. With this amount of power, the bulb won't illuminate at all.

The above explanation goes with other loads too. With 0.25 per-unit power, refrigerator's motor can't compress the gas and even can't get started. That why this paper is set operational voltage limitations for both critical and non-critical loads. All the gathered references in this paper have neglected this problem. In this paper, the minimum and maximum voltage limitation for non-critical load are set at 0.8 and 1.2 per-unit. But it could be another number depends on the type of load and its performance.

A brief comparison between the proposed electric spring and pervious works is shown in Table I. The paper [31] has employed the ES with reactive power compensation in an islanded microgrid. The aim of this control strategy is to regulate voltage of critical load and let the non-critical load to fluctuate. Paper [34] has used several electric springs with reactive power compensation in a distribution network (grid-connected). The aim of [34] is a coordinated voltage regulation for critical loads. The paper [41] has utilized the ES with active and reactive power compensations in an islanded microgrid. The aim of this control strategy is voltage regulation of critical load and frequency regulation of the microgrid. The proposed ES in this paper is based on active and reactive power compensations in microgrid in grid-connected mode. The proposed strategy can control voltages of both critical and non-critical loads.

3. ES Voltage Regulation

3.1.ES Configuration and Operational principle

Fig. 1 shows the structure of an ES. The ES is in series with a non-critical load. The non-critical load includes an individual load or aggregated loads. The phasor summation of non-critical load voltage (v_o) and compensation voltage (v_{es}) is equal to the supply voltage (v_s). A half -bridge power inverter can be implemented for the ES for a single-phase system as shown in Fig. 2. The loads can be classified into two groups: the non-critical load Z_0 and the critical load Z_1. The rule of electric spring is to adjust the voltage of critical load. Let's assume the P_{in} is the sum of the power generator and the intermittent wind generator. The equation (1) is the power balance equation of system in Fig. 1.

$$P_{in} = P_0 + P_1 \;\Rightarrow\; P_{in} = \left(\frac{V_s - V_{es}}{Z_0}\right)^2 Re(Z_0) + \left(\frac{V_s}{Z_1}\right)^2 Re(Z_1) \qquad (1)$$

For simplicity, the loads' type is considered to be resistive therefore;

$$P_{in} = \frac{(V_s - V_{es})^2}{R_0} + \frac{{V_s}^2}{R_1} \qquad (2)$$

where v_0, v_s and v_{es} respectively are voltage phasors of non-critical/critical load (main voltage), and electric spring. The Re is the real term of impedance. The electric spring can work with any type of critical and non-critical loads; resistive, inductive and capacitive.

If the input power (P_{in}) is decreased. The ES regulates the mains voltage (v_s) to reference value (one per-unit). In this situation P_1 remains constant and P_0 is decreased. Actually, voltage of ES (v_{es}) increases until the both sides of power balance equation (1) become equal. Therefore, the non-critical load follows the power generation profile while critical load power is constant.

The equation (3) specifies the electric spring voltage vector under both capacitive and inductive modes.

$$v_{es} = \begin{cases} -v_c & for\ capacitive\ mode \\ +v_c & for\ inductive\ mode \end{cases} \quad (3)$$

where v_c is the voltage of the filter capacitor of the half- bridge inverter.

3.2.Voltage Regulation of Critical and Non-Critical Loads

A typical microgrid with a local wind turbine in the grid-connected mode is shown in Fig. 3. The loads that can be operated with some degree of voltage fluctuations are classified in the non-critical load. All the critical loads are associated to one feeder and all the non-critical loads are connected to another feeder through an electric spring. Actually, each load in Fig. 3 is the summation of parallel loads with same type. The inverter and PWM can be modeled as a variable voltage source [30] which can generate voltage with any amplitude and angle by the controller signal. The switch S is a bypass switch. Just when the critical voltage is normal (for example around 1pu) this switch bypasses the ES and other times it is opened. The microgrid is connected to the upper power system at the point of common coupling (PCC) through line 1 (R_1 , L_1). The wind turbine is connected to point of PCC and the PCC is connected to microgrid by line 2.

The vector diagrams of the ES in a microgrid for three operating modes of a noncritical resistive-inductive load have been illustrated in Fig. 4(a)–4(c). In these figures, the radius of the circle shows the rated main voltage, i.e., 220 V as one per-unit. The rotation direction of the phasors is assumed to be anticlockwise with the frequency of 50 Hz. In grid-connected mode, power variation of microgrid can't change the power system frequency. But the power variation (active and reactive) in the microgrid can change the mains voltage. Fig. 4(a) represents the situation once the ES is in the "neutral" point wherein $v_{es} = 0$ implying that the wind power generation (or any other renewable source) is enough to feed the loads and simultaneously it maintains the main voltage at one per-unit, i.e., the reference value.

When power generation of wind turbine is decreased or power consumption of loads is increased, the voltage drop is happened in the microgrid. The Fig. 4(b) depicts the situation when power generation of wind turbine is decreased and a voltage drop is occurred. For voltage regulation, a reduction in power consumption of non-critical load is required to overcome the voltage drop. Hence, the ES produces a voltage which leads the non-critical load current i_0 by 90°. The ES increases the v_{es} until the vectoral sum of the v_0 and v_{es} becomes one per-unit. According to equation (1), the second term is remained constant but the first term is decreased to keep the power balanced. That means the power of noncritical load must decreases to regulate the mains voltage to 1pu.

When power generation of wind turbine is increased or power consumption of loads is decreased, the voltage increment is occurred. This situation is shown in the Fig. 4(c) which electric spring has increased the voltage of non-critical load. To maintain the power balanced and regulate the main voltage to 1pu, the power consumption of the noncritical load is increased by increasing its voltage.

Fig. 5 depicts the operating modes of the ES for a resistive noncritical load within a grid-a connected microgrid. In resistive load i_0 and v_0 have the same phase angles and here only v_0 is depected. Fig. 4(b) is a situation when power generation of the wind turbine is decreased. For voltage regulation, the reactive power compensation is required. In this situation the ES should produce reactive power (capacitive mode) to boost the mains voltage. Hence, the ES produces a voltage v_{es} which lags the non-critical load current i_0 by 90°. Furthermore, this voltage of ES reduces the voltage and power of noncritical load. Fig. 4(c) is a situation when power generation of wind turbine and mains voltage are increased. In this situation the ES should consume reactive power (inductive mode) to reduce the mains voltage. Hence, the ES produces a voltage v_{es} which leads the non-critical load current i_0 by 90°. The interesting point in resistive load is that the

noncritical voltage v_0 is reduced in both compensation modes (capacitive and inductive). This point could be seen in Fig. 5 (b) (capacitive) and in Fig. 5 (c) (inductive).

If a small voltage drop is occurred, the ES should inject a small reactive power by producing a small voltage (v_{es}) as it is shown in Fig. 6(a). If a medium voltage drop is occurred the ES should produce a medium voltage (v_{es}) to regulate the mains voltage as it is shown in Fig. 6(b). When ES voltage (v_{es}) is increased the noncritical load voltage (v_0) is decreased. For compensating a big voltage drop the noncritical load voltage (v_0) is decreased significantly. Very small noncritical load voltage (v_0) is inefficient for many operations (motors couldn't start, bulbs couldn't illuminate and etc.).

With reactive power compensation, the v_s is 1pu and the v_0 in Fig. 7(a) is 0.5pu which is lower than its operational limit (0.8pu). Let's divide vector of v_{es} to v_q and v_p. The v_q is the voltage of ES which varies reactive power (capacitive or inductive). The v_p is the voltage of ES which injects or absorbs active power. For increasing noncritical voltage, the ES should produce a v_p voltage with 180° phase angle difference with non-critical load current i_0 or v_0 (in resistive load). For compensating voltage and power of non-critical load the ES should inject active power. The Fig. 7(a) and 7(b) are shown vector diagram of voltages before and after active power injection. As it is shown in Fig. 7, with active power injection, the mains voltage v_s is not changed only the v_0 is increased. Obviously, for decreasing the v_0 ,the ES should produce a voltage v_p having same phase angle with non-critical load current i_0. Therefore, the ES can regulate critical load voltage with reactive power compensation and regulate non-critical load voltage with active power compensation. This double voltage control is possible in grid-connected microgrid or active distribution network. But in islanded microgrid, active power compensation changes the microgrid frequency.

4. The Proposed Control Strategy

4.1.Electric spring power circuit and modeling

Fig. 8 illustrates the block diagram of the test system. For the sake of simplicity, both critical and non-critical loads are considered to be resistive. The controller controls the voltage vector v_{es} which is sum of v_q and v_p.

The power circuit of the Electric Spring is shown in Fig. 9. The v_{es} represents the voltage provided by the ES and L_f, R_f and C_f are the inductance and internal resistance of inductor and capacitor of the output filter at the inverter terminal.

It is noted that in this configuration, the capacitor should be protected by means of a LC filter. The state space averaged model of inverter is not proofed in this paper, the details can be found in [43] and [44]. The averaged circuit model is shown in Fig. 9.

The reactance of the filter capacitor C_f is large enough in the frequency of 50 Hz. The v_a is the output voltage of inverter before the filter (is shown in Fig. 9). The v_{es} and v_a are almost in phase.

Two DC source are used in the half bridge inverter of the ES. The DC voltage is 480 V which made of two 240 V DC sources. The DC source could be any bidirectional DC power source or batteries with an ac/dc converter to charge or discharge the batteries in active power compensation. There is no need for any bidirectional DC source or storage in reactive power compensation.

The critical loads are voltage sensitive and when the voltage fluctuates the voltage protection system may trip the loads. The power protection system would disconnect the microgrid from the grid, when the power consumption of the microgrid is higher than the generated power of the grid. When there is a smart load (ES series with noncritical load) in the microgrid, the ES regulates the grid voltage and lets the non-critical load voltage to fluctuate dynamically. Actually, the ES regulates the grid voltage and automatically shape the load power to follow the generated power.

With this operation, the ES actually stabilizes the power grid so, the protection systems (voltage protection and power protection) don't trip the microgrid. Ref. [34] is demonstrated the stability improvement of distribution network by using electric spring.

4.2.The Proposed Controller

Fig. 10 illustrates the proposed controller. As shown to control the voltage of both critical and non-critical loads, two separated closed-loop controllers are needed for the ES. The voltage of the critical load is adjusted by reactive power compensation or the v_q control loop. At first of the v_q control loop, there is a Gain block with $1/V_{ref}$ gain value. The input voltage (V_s) multiplies in the gain value to limit the magnitude and convert it to the per-unit scale V_s^{pu}.The error signal enters to PI controller. The roles of PI here are to accelerate the output response and to remove the steady state error. Then the control signal enters to a saturation block with 1 and -1 upper and lower limits.

The block above the PLL is a sequence block which calculates the phasor values of the input signal (i_0) and here just the angle (θ) is needed. The PLL block determines the frequency and the fundamental component of signal phase angle. The PLL block models a Phase Lock Loop (PLL) closed-loop control system, which tracks the frequency and phase of a sinusoidal signal by using an internal frequency oscillator. The control system adjusts the internal oscillator frequency to keep the phases difference to 0. With a PLL block the ωt of the noncritical load current (i_0) is obtained. The sequence block gives the angle (θ) of i_0 therefore, the ($\omega t + \theta$) of i_0 is achieved. The v_q should be perpendicular to i_0 for reactive power compensation. That's why $\pi/2$ must add to angle of i_0.

The maximum output voltage of the half-bridge inverter is related to capacitor's voltage. Each capacitor is charged to half of battery voltage ($V_{DC}/2$). The V_{DC} is 480 V and the maximum output of the inverter is 240 V. Then, the sine wave $240Sin(\omega t + \theta - \pi/2)$ is made.

The v_q is the multiplication of sine wave with output value of saturation block (between -1 to 1). If the value of saturation block is positive the controller works in the capacitive compensation mode, and if it is negative the controller works in the inductive compensation mode.

The non-critical load voltage is regulated by active power compensation or the v_p control loop. Whenever the voltage V_0^{pu} is lower than 0.8pu or upper than 1.2pu the ES works as an active compensator to regulate the non-critical voltage. If the V_0^{pu} goes lower than 0.8pu the value of error e_1 becomes positive. The limits of saturation block S_1 are 0 and 1 (positive). Therefore, when the V_0^{pu} is higher than 0.8pu the saturation block e_1 is negative but when it is lower than 0.8pu, the e_1 is positive and the PI controller operates. If the V_0^{pu} goes higher than 1.2pu the value of error e_2 becomes negative. The saturation block S_2 allows just negative values to pass (-1 to 0). When the V_0^{pu} is lower than 1.2pu the saturation block e_2 is positive and when it is higher than 1.2pu, the e_2 is negative and the PI controller operates. The saturated blocks outputs S_1 and S_2 are added and the point here is when one of the outputs has a value the another one's value is zero. That means ES can work in one mode in each time. The controller works when the V_0^{pu} is lower than 0.8pu or higher than 1.2pu. When the PI output is positive that means, a voltage drop is taken place and an active power injection is needed. This positive value multiplies in $240Sin(\omega t + \theta - \pi)$ to make the v_p. When the PI output is negative that means, a voltage increment is taken place and an active power absorption is needed to decrease the voltage. This negative value multiplies

in $240Sin(\omega t + \theta - \pi)$ to make the v_p. The output signal is v_{es} which is the sum of the v_q and v_p. The non-critical voltage is regulated on its boundaries 0.8pu or 1.2pu not 1pu.

5. Experimental Results

The experimental results of implementing the proposed strategy in a microgrid in grid-connected mode have been addressed in this section. Fig. 17 is the experimental setup for testing the ES with the proposed control strategy. The microgrid has 3-phases and the ES is situated in the phase A For producing voltage reduction and voltage increment scenarios, the reactive power (injecting or absorbing) of renewable source is changed.

In the first scenario the reactive power consumption of renewable is increased from 0 to 1000Var, consequently 3 percent voltage reduction is taken place. Fig. 11 (a) shows the mains voltages V_s^{pu} in phase A with ES and another phase without ES. Fig. 11 (b) demonstrates the voltages of critical load V_s^{pu} , non-critical load V_0^{pu}, and electric spring V_{es}^{pu}. With 0.3pu voltage injection of ES the mains voltage is regulated. The voltage of non-critical load V_0^{pu} is reached to 0.9pu which is above its operational limit, and the ES operates in reactive power compensation mode (capacitive).

In the second scenario, the reactive power injection of renewable is increased from 0 to 700Var, consequently 2 percent voltage increment is taken place. Fig. 12 (a) shows the mains voltages V_s^{pu} with ES and without ES. As it can be seen in Fig. 12 (b), with 0.3pu voltage injection of ES the mains voltage is regulated. The voltage of non-critical load V_0^{pu} is reached to 0.9pu which is above its operational limit, and the ES operates in reactive power compensation mode (inductive).

In the third scenario, the reactive power injection of renewable is increased from 0 to 1200Var, consequently, 4 percent voltage increment is taken place (is shown in Fig. 13). Both voltages of non-critical load V_0^{pu}, and electric spring V_{es}^{pu} are almost equal (about 0.7pu). The 0.7pu voltage

for non-critical load V_0^{pu} is lower than its operational limit (0.8pu). In this scenario the ES operates just in reactive power compensation mode.

In the fourth scenario, ES operates in both active and reactive mode for the same voltage increment of the third scenario. The result of the proposed control strategy is shown in Fig. 14. The ES with injecting active power regulates the voltage of non-critical load. The voltage diagram in Figs. 15 and 16 are the results of fifth scenario respectively with the conventional control strategy (just reactive) and the proposed control strategy. In the fifth scenario the reactive power consumption of renewable is increased from 0 to 2200Var. The 6% voltage drop is taken in both Figs but the proposed control strategy regulates the noncritical voltage on 0.8 pu.

The specification of experimental setup is shown in Table II. The Electric spring is set in one phase (A) of three-phase system. The critical and non-critical loads are selected to be equal to see the effect of non-critical load on the critical load voltage regulation fairly. The PI parameters can be chosen by Matlab optimization or experimentally. Actually, the PI block in Simulink has a "Tune" function which can automatically gains the Kp, Ki and Kd (in PID). Designing LC filter in Matlab/Simulink is easy by using "Filter Design and Analysis" tool. But in experimental test an expert is really needed because the situation may be different a little bit in reality. The renewable power source is a P-Q controllable power source. This source is made of a DC power source and a DC to AC converter to be able to generate any active and reactive power. For producing the voltage fluctuation, the reactive power should be changed from -2500Var (Inductive mode) to 2500 Var (capacitive mode). In the distribution networks the voltage is regulated mostly by reactive power because the active power has a very low effect on the voltage regulation. That's why the voltage of this experiment is changed by reactive power changing of the P-Q controllable power source.

The proposed control strategy is very simple and effective. The v_{es} is divided into two phasors, v_q and v_p. Each vector is controlled by a simple closed loop control. The needed battery or any DC source for the ES is very small. Because, firstly the reactive power compensation doesn't need any DC source. It just consumes a very small amount of power for switching and capacitor losses. Secondly, the ES rarely produces the active power. Just whenever the non-critical load voltage goes below the 0.8pu, the ES produces the active power. Thirdly, when the ES works in active power compensation, it just produces a small amount of active power to reach the noncritical voltage to 0.8pu (operational limit in this paper).

6. Conclusions

In this paper, a simple double voltage control is proposed for the electric spring to control both critical and non-critical voltage with variable and uncertain renewables. The biggest disadvantage of the conventional electric springs is to let the noncritical load power fluctuate with no limitation. In voltage drop scenario, a conventional ES decreases the non-critical voltage to boost the voltage of critical load. Even though the noncritical loads can tolerate some sort of voltage deviation but they cannot work under any voltage deviation, especially motor-based loads. The proposed ES regulates the critical voltage on a fixed voltage while lets the non-critical voltage fluctuate between a limitation (for example 0.8pu to 1.2pu). The limitation is depended on the operational limits of the load. The ES supports the voltage in both upward and downward corrections for both loads in microgrids or active distribution networks. Furthermore, with the proposed control strategy the needed battery or DC source for the ES is very small. The proposed control strategy is validated by experimental results. Results from different scenarios show that with the proposed strategy the ES can effectively mitigate double voltage control and power factor correction while dynamically managing the demand response of the system at the same time.

Acknowledgment

J.P.S. Catalão acknowledges the support by FEDER funds through COMPETE 2020 and by Portuguese funds through FCT, under POCI-01-0145-FEDER-029803 (02/SAICT/2017).

References

[1] P. P. Varaiya, F. F. Wu, and J. W. Bialek, "Smart operation of smart grid: Risk-limiting dispatch," *Proc. IEEE*, vol. 99, no. 1, pp. 40–57, 2011.

[2] H. Fallahzadeh-Abarghouei, S. Hasanvand, A. Nikoobakht, M. Doostizadeh, "Decentralized and hierarchical voltage management of renewable energy resources in distribution smart grid," *International Journal of Electrical Power & Energy Systems*, Vol. 100, pp. 117-128, Sept. 2018

[3] M. Yilmaz, R. El-Shatshat, "State-based Volt/VAR control strategies for active distribution networks," *International Journal of Electrical Power & Energy Systems*, Vol. 100, pp. 411-421, Sept. 2018

[4] M. Aragüés-Peñalba, J. S. Bassols, S. G. Arellano, A. Sumper, O. G. Bellmunt, "Optimal operation of hybrid high voltage direct current and alternating current networks based on OPF combined with droop voltage control," *International Journal of Electrical Power & Energy Systems*, Vol. 101, pp. 176-188, Oct. 2018

[5] G-H. Gwon, C.-H. Kim, Y-S. Oh, C-H. NohT-H. Jung, J. Han, "Mitigation of voltage unbalance by using static load transfer switch in bipolar low voltage DC distribution system," *International Journal of Electrical Power & Energy Systems*, Vol. 90, pp. 158-167, Sept. 2017

[6] M. M. Rahman, A. Arefi, G. M. Shafiullah, S. Hettiwatte, "A new approach to voltage management in unbalanced low voltage networks using demand response and OLTC considering consumer preference," *International Journal of Electrical Power & Energy Systems*, Vol. 99, pp. 11-27, July 2018

[7] D. Westermann and A. John, "Demand matching wind power generation with wide-area measurement and demand-side management," *IEEE Trans. Energy Conversion*, vol. 22, no. 1, pp. 145–149, 2007.

[8] P. Palensky and D. Dietrich, "Demand side management: Demand response, intelligent energy systems, and smart loads," *IEEE Trans. Ind. Informatics*, vol. 7, no. 3, pp. 381–388, 2011.

[9] A. Mohsenian-Rad, V. W. S. Wong, J. Jatskevich, R. Schober, and A. Leon-Garcia, "Autonomous demand-side management based on gametheoretic energy consumption scheduling for the future smart grid," *IEEE Trans. Smart Grid*, vol. 1, no. 3, pp. 320–331, Dec. 2010.

[10] M. Parvania and M. Fotuhi-Firuzabad, "Demand response scheduling by stochastic SCUC," *IEEE Trans. Smart Grid*, vol. 1, no. 1, pp. 89–98, Jun. 2010.

[11] M. Pedrasa, T. D. Spooner, and I. F. MacGill, "Scheduling of demand side resources using binary particle swarm optimization," *IEEE Trans. PowerSyst.*, vol. 24, no. 3, pp. 1173–1181, Aug. 2009.

[12] A. J. Conejo, J. M. Morales, and L. Baringo, "Real-time demand response model," *IEEE Trans. Smart Grid*, vol. 1, no. 3, pp. 236–242, Dec. 2010.

[13] A. Mohsenian-Rad and A. Leon-Garcia, "Optimal residential load control with price prediction in real-time electricity pricing environments," *IEEE Trans. Smart Grid*, vol. 1, no. 2, pp. 120–133, Sep. 2010

[14] A. J. Roscoe and G. Ault, "Supporting high penetrations of renewable generation via implementation of real-time electricity pricing and demand response," *IET Renewable Power Generat.*, vol. 4, no. 4, pp. 369–382, Jul. 2010.

[15] F. Kienzle, P. Ahcin, and G. Andersson, "Valuing investments in multi-energy conversion, storage, and demand-side management systems under uncertainty," *IEEE Trans. Sustainable Energy*, vol. 2, no. 2, pp. 194–202, Apr. 2011

[16] S. C. Lee, S. J. Kim, and S. H. Kim, "Demand side management with air conditioner loads based on the queuing system model," *IEEE Trans. Power Syst.*, vol. 26, no. 2, pp. 661–668, Sep. 2010.

[17] G. C. Heffner, C. A. Goldman, and M. M. Moezzi, "Innovative approaches to verifying demand response of water heater load control," *IEEE Trans. Power Del.*, vol. 21, no. 1, pp. 388–397, Jan. 2006.

[18] A. Brooks, E. Lu, D. Reicher, C. Spirakis, and B. Weihl, "Demand dispatch," *IEEE Power Energy Mag.*, vol. 8, no. 3, pp. 20–29, May/Jun. 2010.

[19] Y. Wang, Y. Li, Y. Tan, and J. Han, "Hybrid AC/DC microgrid architecture with comprehensive control strategy for energy management of smart building," *International Journal of Electrical power & Energy Systems*, vol. 101, pp. 151–161, Oct. 2018.

[20] A. K. Hasan, D. Chowdhury, and M. Z. Rahman Khan, "Scalable DC microgrid architecture with a one-way communication-based control interface," *International Con. On Electrical and Computer Eng.*, Dec. 2018.

[21] D. Chowdhury, A. K. Hasan, and M. Z. Rahman Khan, "Scalable DC microgrid architecture with phase shifted full bridge converter-based power management unit," *International Conference on Electrical and Computer Eng.*, Dec. 2018.

[22] A. K. Hasan, D. Chowdhury, and M. Z. Rahman Khan, "Performance analysis of a Scalable DC microgrid offering solar power-based energy access and efficient control for domestic loads," *Electrical Engineering and systems science, signal processing*, Jan. 2018.

[23] S. Y. M. Mousavi, A. Jalilian, M. Savaghebi, and J. M. Guerrero, "Coordinated control of multifunctional Inverters for voltage support and harmonic compensation in a grid connected microgrid," *Electric Power Systems Research*, vol. 155, pp. 254–264 Feb. 2018.

[24] M. Kashif, M. J. Hossain, F. Zhuo, and S. Gautam, "Design and implementation of a three-level active power filter for harmonic and reactive power compensation," *Electric Power Systems Research*, vol. 165, pp. 144–156 Dec. 2018.

[25] O. B. Adewuyi, R. Shigenobu, K. Ooya, T. Senjyu, and A. M. Howlader, "Static voltage stability improvement with battery energy storage considering optimal control of active and reactive power injection," *Electric Power Systems Research*, vol. 172, pp. 303–312, July 2019.

[26] Q. Liu, Y. Li, L. F. Luo, and Y. Peng, "Power quality management of PV power plant with transformer integrated filtering method," *IEEE Transaction on Power Delivery*, vol. 34, Issue 3, pp.941-949, Nov. 2018.

[27] S. Das, K. M. Salim, and D. Chowdhury, "A novel variable width PWM switching based buck converter to control power factor correction phenomenon for an efficacious grid integrated electric vehicle battery charger," *TENCON 2017I EEE Region 10 conference*, Dec. 2017.

[28] D. Chowdhury, M. I. Hussain, Md. G. Zakaria, Md. Z. Rahman Khan, and M. Z. Haider, "An electrically isolated low power LED driver offering power factor correction with ameliorated mains current THD," *2018 8th India International conference on power electronics*, May. 2019.

[29] A. Benyamina, S. Moulahoum, I. Colak, and R. Bayindir, "Design and real time implementation of adaptive neural-fuzzy inference system controller-based unity single phase power factor converter," *Electric Power Systems Research*, vol. 152, pp. 357–366 Nov. 2017.

[30] S. Y. R. Hui, C. K. Lee, and F. F. Wu, "Electric springs—a new smart grid technology," *IEEE Trans. Smart Grid*, vol. 3, no. 3, pp. 1552–1561, Sep. 2012.

[31] J. Soni and S. K. Panda, "Electric spring for voltage and power stability and power factor correction," *IEEE Trans. Industry Application*, vol. 53, no. 4, pp. 3871–3879, Mar. 2017.

[32] Y. Shuo, S. C. Tan, C. K. Lee and S. Y. R. Hui, "Electric spring for power quality improvement," *Applied Power Electronic Conference*, April 2014.

[33] K. T. Mok, M. H. Wang and S. Y. R. Hui, "DC electric springs-An emerging technology for DC grids," *Applied Power Electronic Conference*, May 2015.

[34] C. K. Lee, N. R. Chaudhuri, B. Chaudhuri and S. Y. R. Hui, "Droop Control of distributed electric springs for stabilizing future power grid," *IEEE Trans. Smart Grid*, vol. 4, no. 3, pp. 1558–1566, Sep. 2013.

[35] X. Chen and Y. Hou,"Distributed control of multiple electric springs in microgrids," *Power & Energy Society General Meeting*, Oct. 2015.

[36] X. Luo, Z. Akhtar, C. K. Lee, B. Chaudhuri, S. C. Tan and S. Y. R. Hui, "Distributed Voltage Control with electric springs: comparison with STATCOM," *IEEE Trans. Smart Grid*, vol. 6, no. 1, pp. 209–219, Aug. 2014.

[37] S. Yan, S. C. Tan, C. K. Lee, B. Chaudhuri and S. Y. R. Hui, “Electric spring for reducing power imbalance in three phase power system,” *IEEE Trans. Power Electronics*, vol. 30, no. 7, pp. 3601–3609, Aug. 2014.

[38] T. Yang, K. T. Mok, S. C. Tan and S. Y. R. Hui, “Control of electric springs with coordinated battery management,” *Energy Conversion Congress and Exposition (ECCE*, Oct. 2015.

[39] T. Yang, K. T. Mok, S. C. Tan, C. K. Lee and S. Y. R. Hui, “Electric Springs with coordinated battery management for reducing voltage and frequency fluctuations in microgrids,” *IEEE Trans. Smart Grid*, vol. PP, no. 99, pp. 1–1, Aug. 2016.

[40] C. K. Lee and S. Y. R. Hui, “Reduction of energy storage requirements in future smart grid using electric springs,” *IEEE Trans. Smart Grid*, vol. 4, no. 3, pp. 1282–1288, April. 2013.

[41] X. Chen, Y. Hou, S. C. Tan, C. K. Lee and S. Y. R. Hui, “Mitigating Voltage and frequency fluctuation in microgrids using electric Springs,” *IEEE Trans. Smart Grid*, vol. 6, no. 2, pp. 508–515, Mar. 2015.

[42] C. K. Lee, S. N. Li, and S. Y. R. Hui, “A design methodology for smart LED lighting systems powered by weakly regulated renewable power girds,” *IEEE Trans. Smart Grid*, vol. 2, no. 3, pp. 548–554, Sep. 2011.

[43] N. R. Chaudhuri, C. K. Lee, B. Chaudhuri, and S. Y. R. Hui, “Dynamic Modeling Of Electric Springs,” *IEEE Trans. Smart Grid*, vol. 5, no. 5, pp. 2450–2458, Aug. 2014.

[44] S. R. Sanders, "Generalized averaging method for power conversion circuits," *Power Electronics, IEEE Transactions on*, vol. 6, pp. 251-259, 1991.

Table I: The comparison of different control strategies

Control Type	**Reactive Power Compensation**	**Active Power Compensation**	**Critical-Load Voltage Regulation**	**Non-critical LoadVoltage Regulation**
[31]	✓	–	✓	–
[34]	✓	–	✓	–
[41]	✓	✓	✓	–
Proposed ES	✓	✓	✓	✓

Table II: The specification of the experimental test setup

Description	***Parameter***	***Nominal Value***
Load	Critical	50 Ω
	Noncritical	50 Ω
Filter Indicator	L_f	500 µH
Filter Capacitor	C_f	13 µF
PI Controller	K_p & K_I	0.2 & 0.05
Switching Frequency	f_s	20 kHz
Renewable Source (Programmable PQ source)	Active Power	0-5000 W
	Reactive Power	-2500 to 2500 Var

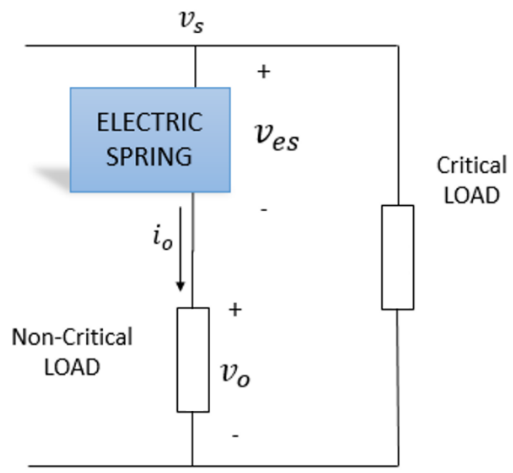

Fig. 1. The circuit block diagram of an ES with critical and non-critical loads

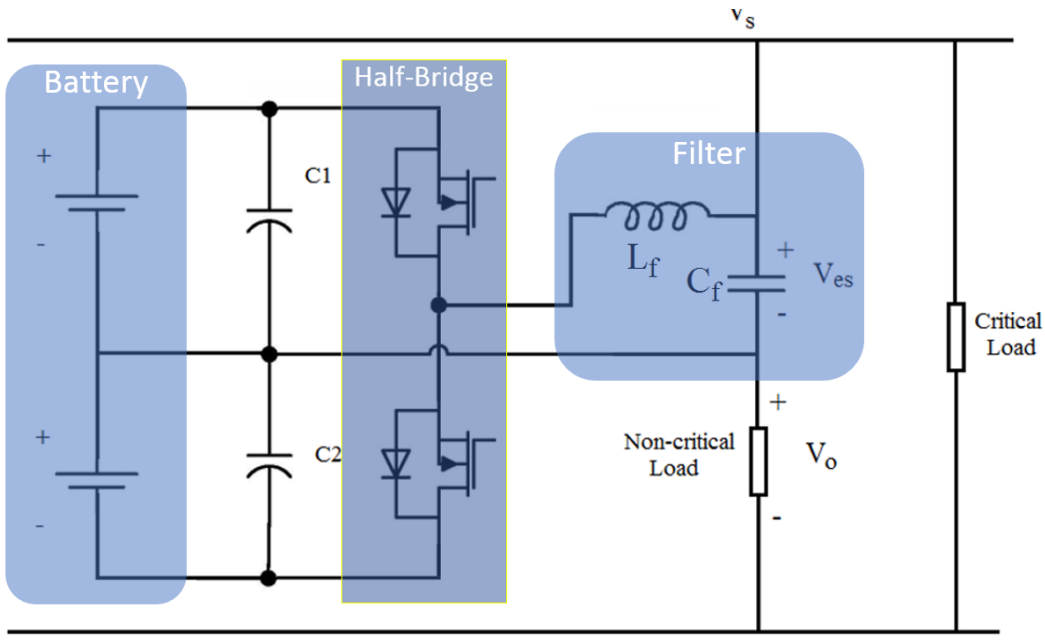

Fig. 2. The half-bridge power inverter utilized in electric spring

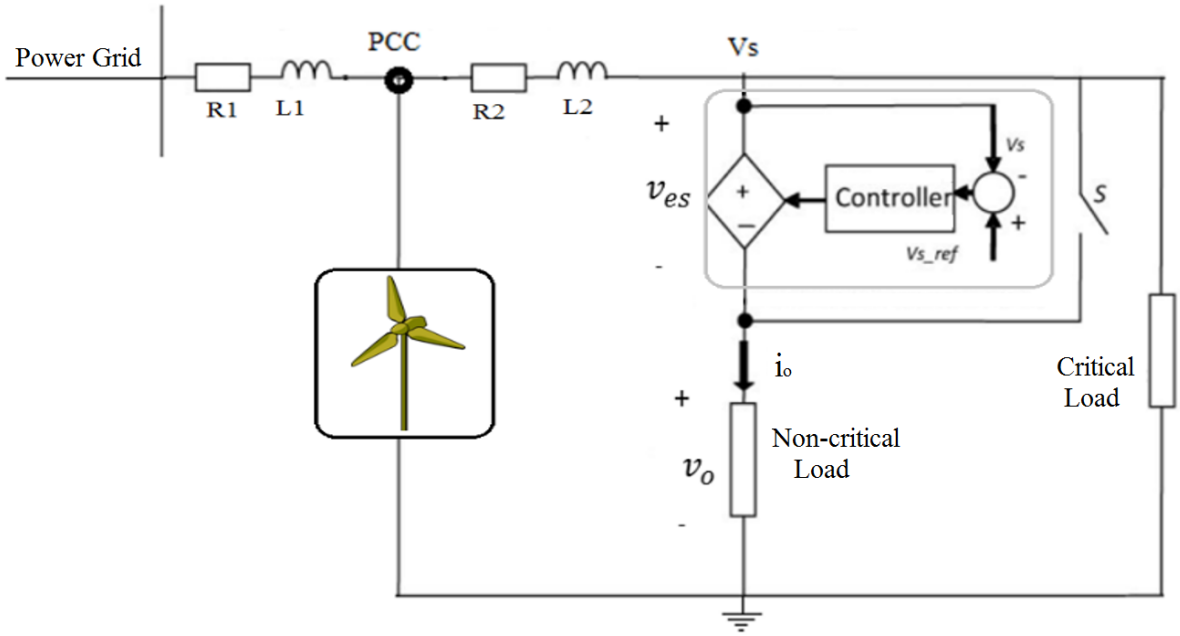

Fig. 3. A typical microgid in grid-connected mode

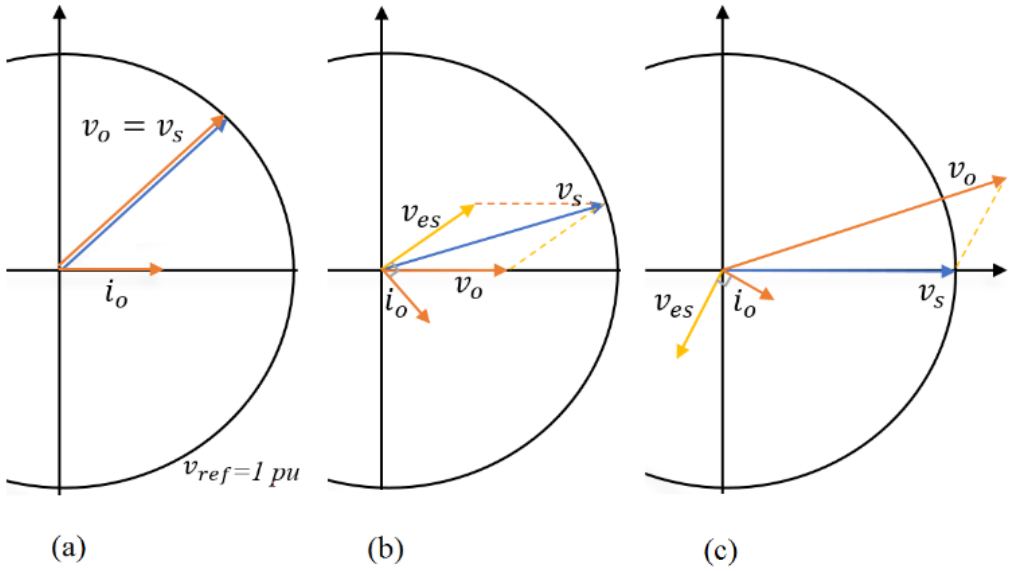

Fig. 4. ES voltage regulation modes for a resistive-inductive noncritical load. (a) Neutral. (b) Inductive mode. (c) Capacitive mode.

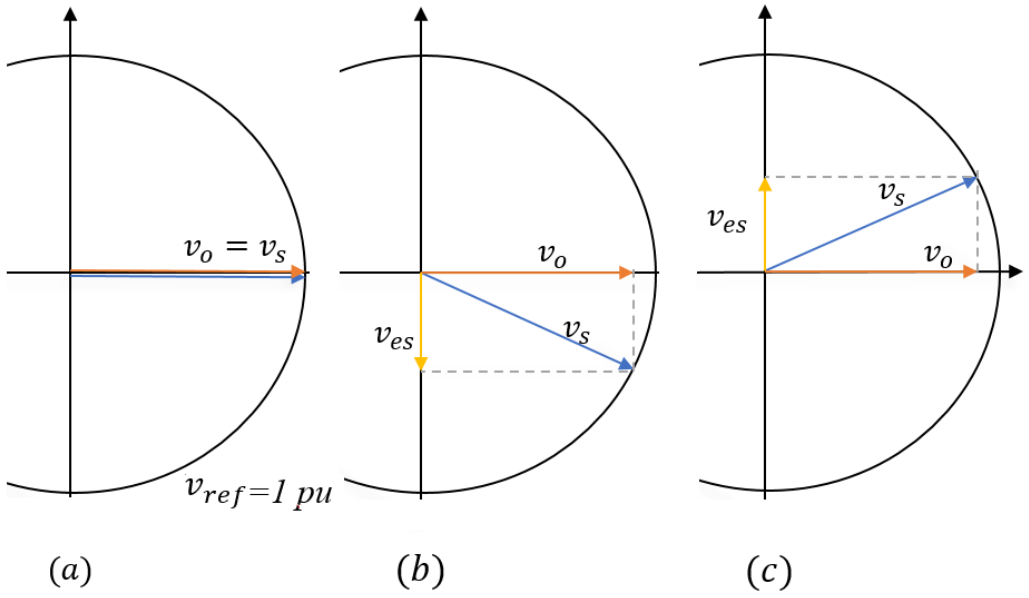

Fig. 5. Operating modes of the electric spring to maintain v_s to 1pu for a resistive noncritical load in a microgrid in grid-connected mode. (a) Neutral. (b) Capacitive mode. (c) Inductive mode

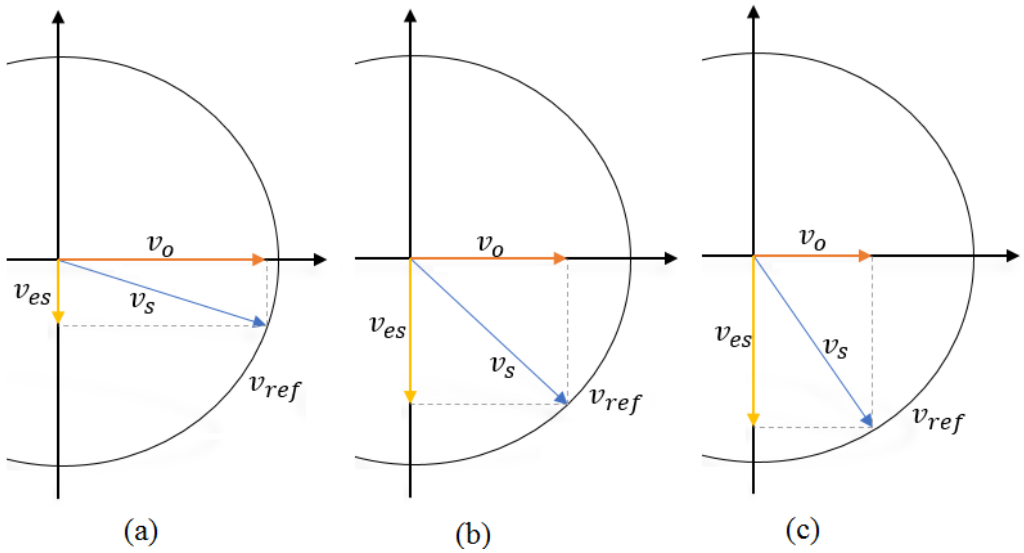

Fig. 6. Vector diagram of voltages with different amplitudes.

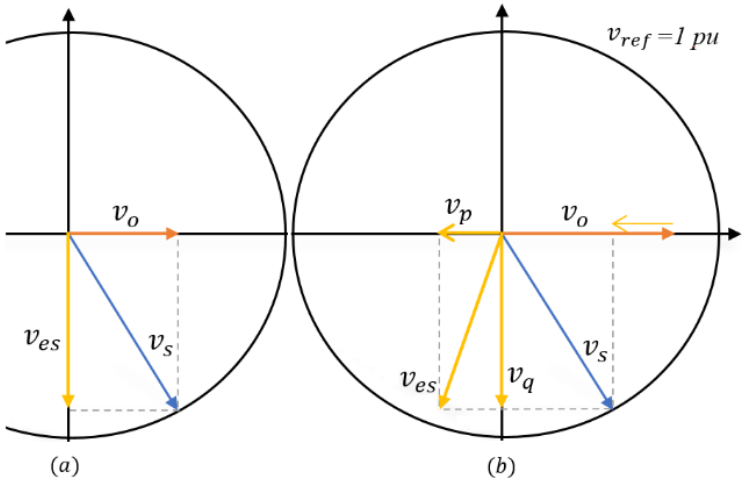

Fig. 7. Voltage vector diagram before (a) and after (b) active power injection.

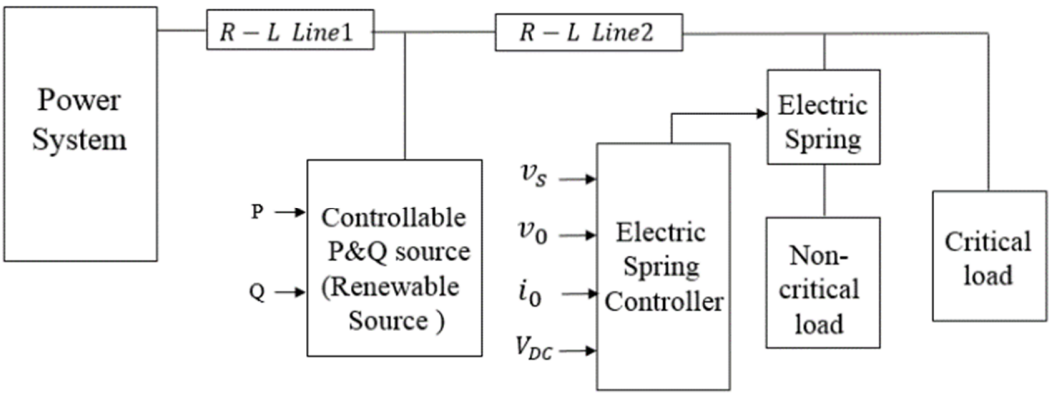

Fig. 8. Block diagram of test system with electric spring.

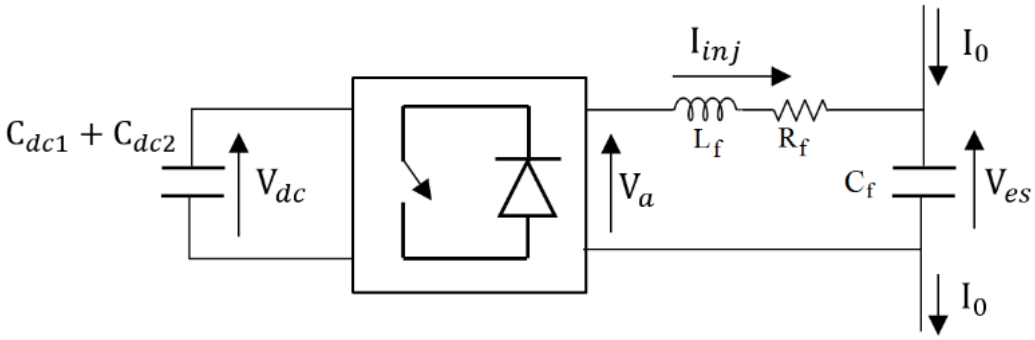

Fig. 9. Power circuit of electric spring [38].

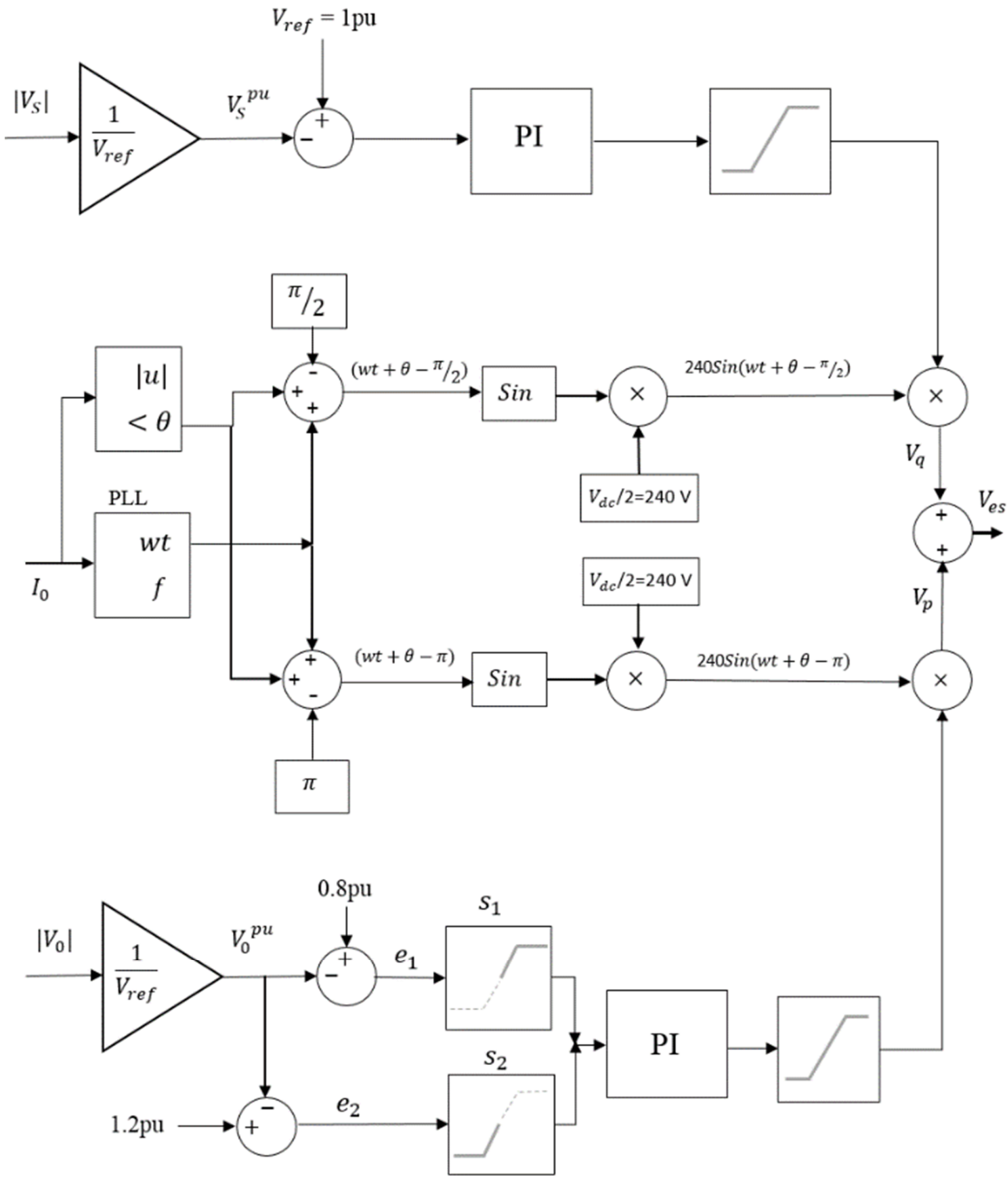

Fig. 10. Block diagram of electric spring controller.

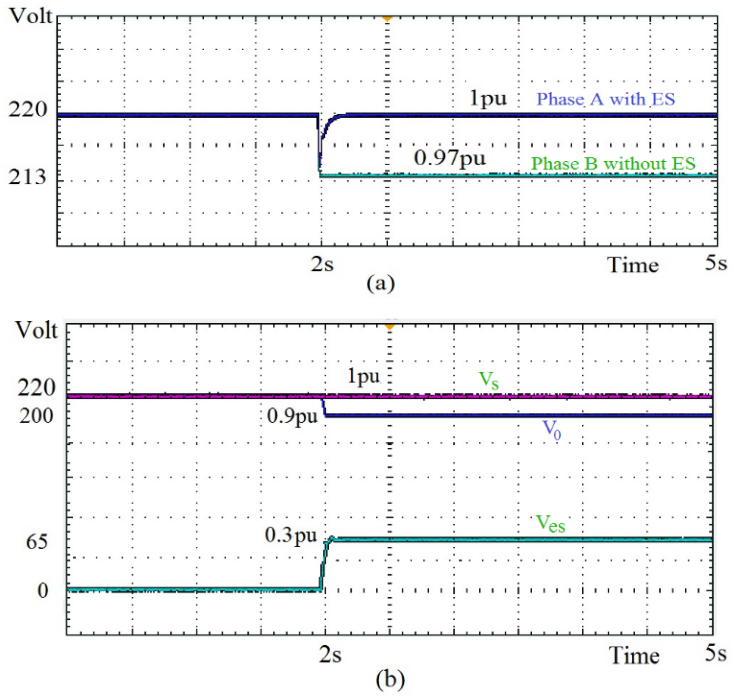

Fig. 11. Reactive power consumption of the renewable is increased from 0 to 1000 Var at t=2.0 s (a) Voltages of phase A with ES and B without ES, (b) Voltages of critical load V_s^{pu} , non-critical load V_0^{pu}, and electric spring V_{es}^{pu}.

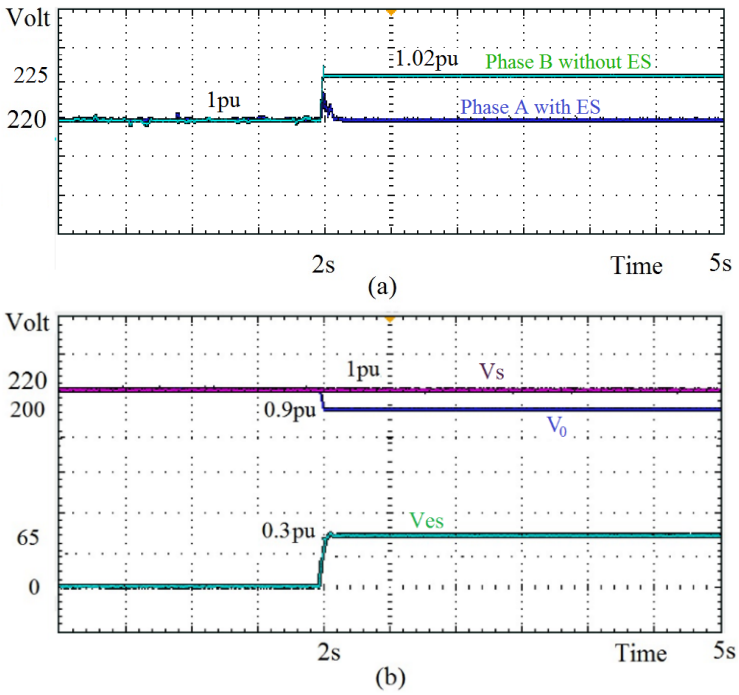

Fig. 12. Reactive power injection of the renewable is increased from 0 to 700 Var at t=2.0 s (a) Voltages of phase A with ES and B without ES, (b) Voltages of critical load V_s^{pu} , non-critical load V_0^{pu}, and electric spring V_{es}^{pu}.

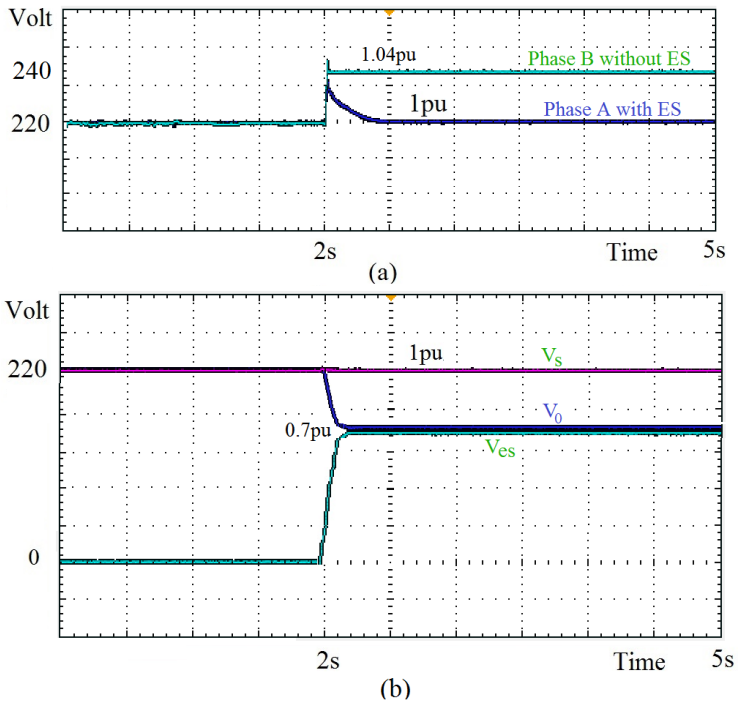

Fig. 13. Reactive power injection of the renewable is increased from 0 to 1200 Var at t=2.0 s (a) Voltages of phase A with ES and B without ES, (b) Voltages of critical load V_s^{pu} , non-critical load V_0^{pu}, and electric spring V_{es}^{pu}.

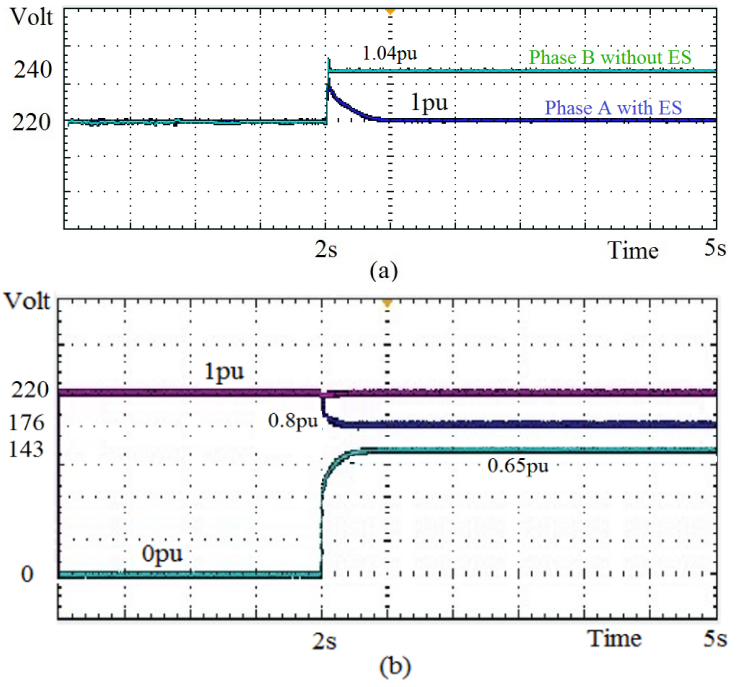

Fig. 14. Reactive power injection of the renewable is increased from 0 to 1200 Var at t=2.0 s (a) Voltages of phase A with ES and B without ES, (b) The voltages of critical load V_s^{pu} , non-critical load V_0^{pu}, and electric spring V_{es}^{pu} with the proposed ccontrol strategy; active and reactive compensation mode.

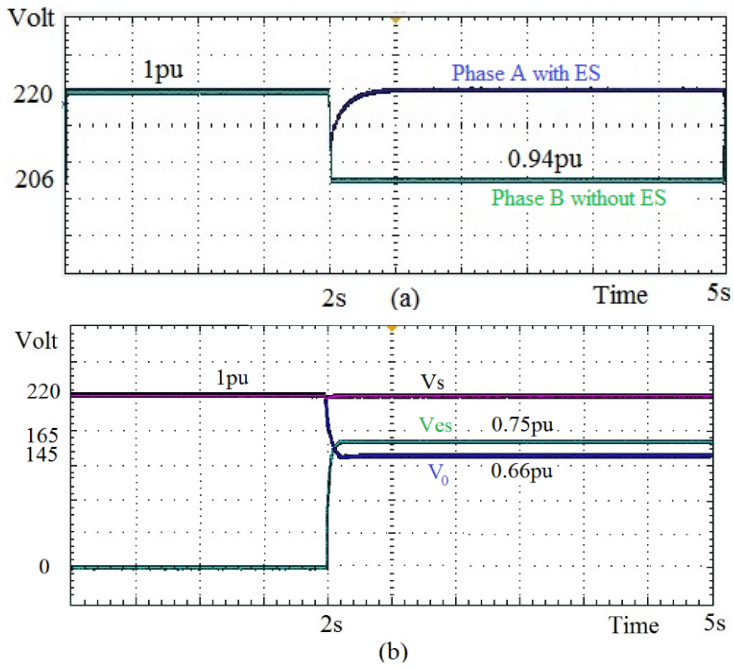

Fig. 15. Reactive power consumption of the renewable is increased from 0 to 2200 Var at t=2.0 s (a) Voltages of phase A with ES and B without ES, (b) voltages of critical load V_s^{pu} , non-critical load V_0^{pu}, and electric spring V_{es}^{pu}.

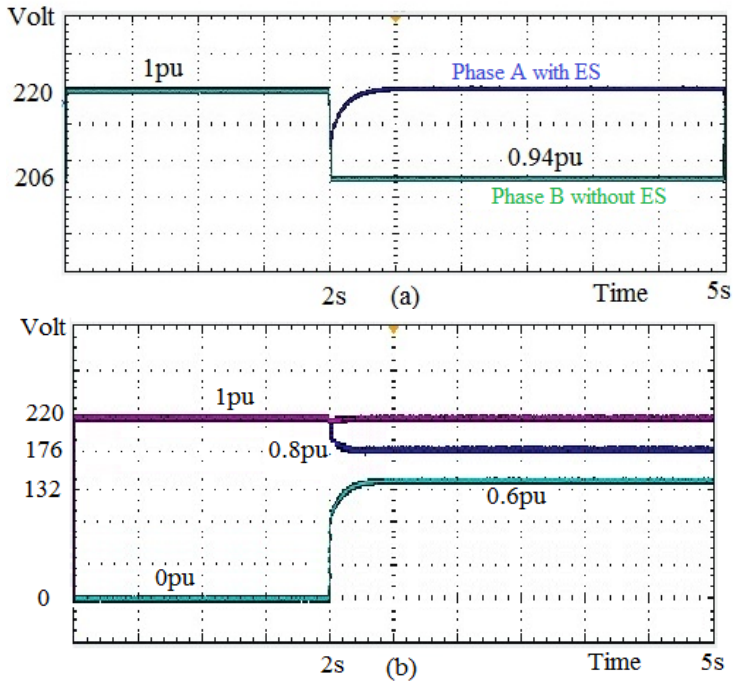

Fig. 16. Reactive power consumption of the renewable is increased from 0 to 2200 Var at t=2.0 s (a) Voltages of phase A with ES and B without ES, (b) The voltages of critical load V_s^{pu} , non-critical load V_0^{pu}, and electric spring V_{es}^{pu} with the proposed ccontrol strategy; active and reactive compensation mode.

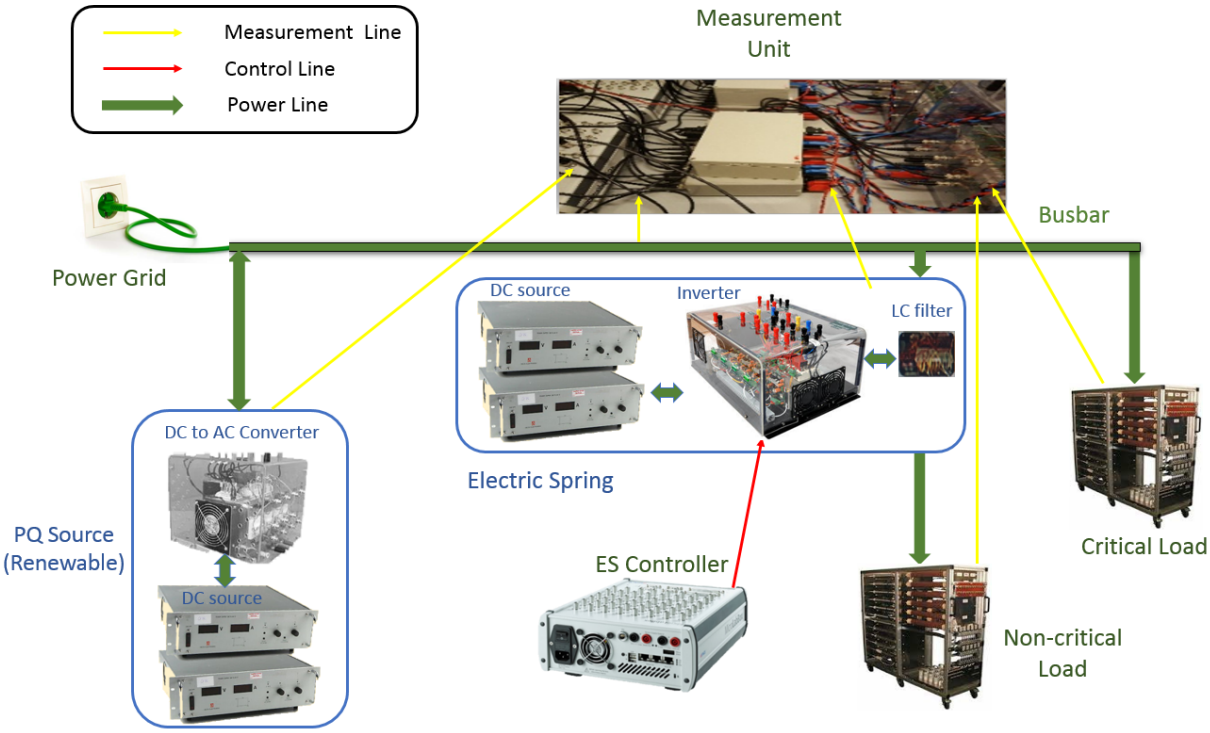

Fig. 17. The experimental setup for testing the electric spring operation with the proposed control strategy